

Hot Corrosion of Ti-Based Intermetallics with Coatings in NaCl+(Na,K)₂SO₄ Melts at 750°C

Yuming Xiong^{*,a}, Xiang Xiong^a, Shenglong Zhu^b and Fuhui Wang^{*,b}

^aState Key Laboratory for Powder Metallurgy, Institute of Powder Metallurgy Research, Central South University, Changsha 410083, China

^bState Key Laboratory for Corrosion and Protection, Institute of Metal Research in Chinese Academy of Sciences, Shenyang 110016, China

Abstract: In this study, the hot corrosion of TiAl, TiAlNb, and Ti₃AlNb intermetallics with or without enamel coating and sputtered TiAlCr coating in (Na, K)₂SO₄ + NaCl melts at 750°C is investigated. The interfacial reaction between enamel and those alloys during hot corrosion has also been evaluated. The results indicate that severe corrosion of bare alloys occurs due to the self catalysis chlorination and sulfidation of metallic components. TiAlNb shows the best corrosion resistance among the three examined alloys. The sputtered TiAlCr coating fails to protect the substrate from hot corrosion due to the rapid volatility of chromium chlorides other than the formation of protective Al₂O₃ scale. The enamel coating could protect Ti-base alloys from hot corrosion due to its thermal stability and matched thermal expansion coefficient with the substrates. However, the interfacial reaction and selective oxidation of aluminum between enamel coating and Ti-alloys substrate under a low oxygen partial pressure decreases the stability of enamel coating with increasing the activity of aluminum of alloys.

Keywords: Titanium aluminides, enamel coatings, hot corrosion.

1. INTRODUCTION

The potential applications of Ti-based intermetallics due to their low density and high specific strength are in aerospace, chemical and petrochemical, metallurgical, and medical industries, where both excellent mechanical properties and high temperature oxidation resistance are required [1-4]. However, the general TiAl alloys show poor oxidation resistance above 800°C due to the similar oxygen affinity of Al and Ti. The Al content should be more than a critical value (~67 at.%) to form a protective scale Al₂O₃ during oxidation [5, 6]. With increasing Al content, however the formation of brittle phases, such as TiAl₂ and TiAl₃, will degrade the mechanical properties of TiAl alloys. Thus, it is important to balance the oxidation resistance and mechanical properties of Ti-based alloys by means of alloying and surface modification. It has been confirmed that the additives of Nb and Cr could markedly improve the oxidation resistance of TiAl alloys without significant loss of mechanical properties [7-14].

Nevertheless, the protective oxides scale on Ti-based alloys would be destabilized due to the formation of an Al-depleted sub-layer during long-term oxidation [14-18]. Many coatings (Al₂O₃, SiO₂, Si₃N₄, aluminides, and MCrAlY) could provide good protection for titanium alloys against oxidation and act as a barrier to reduce the ingress of oxygen at elevated temperature. Recently, we have developed an enamel coating for Ti-based alloys with enhanced resistance

against oxidation and corrosion due to their high thermochemical stability and matching thermal expansion coefficient with Ti-alloy substrate [19-22]. Moreover, the enamel coatings prepared by vitrification are economically more attractive than those coatings (such as TiAlCr and MCrAlY) produced by means of relatively expensive Physical Vapor Deposition (PVD) process.

Moreover, the negative effect of Cl⁻ ion on the protectiveness of metallic coatings from hot corrosion has been argued [22-26]. The corrosion rate of the coatings containing Cr sharply increases due to the formation of volatile chromium chloride. Thus, the enamel coating may be a better candidate than metallic coatings (including TiAlCr) for Ti-based alloys against hot corrosion of salt melts containing Cl⁻ ion, such as a coastal environment. In the present paper, the hot corrosion behavior of enamel coatings and TiAlCr coating on TiAl, TiAlNb and Ti₃AlNb alloys in (Na, K)₂SO₄ + NaCl mixture melts was examined and compared. The compatibility variation of enamel coating with the substrate was evaluated through the study on the interfacial reaction during hot corrosion at elevated temperature.

2. EXPERIMENTAL

2.1. Substrate Materials

The examined alloys Ti-48Al, Ti-46.5Al-5Nb, and Ti-24Al-17Nb-0.5Mo (at.%), which are briefly denoted as TiAl, TiAlNb, and Ti₃AlNb respectively hereinafter, were prepared by melting the high-purity metals in an induction furnace under an argon protective atmosphere, followed by solidification in air in a cylindrical mould, and then the cast alloys were homogenized at 1000°C for 1h. The ingots were sliced into specimens in a dimension of 15×10×3.0 mm,

*Address correspondence to these authors at the State Key Laboratory for Powder Metallurgy, Institute of Powder Metallurgy Research, Central South University, Changsha 410083, China;
E-mails: ymxiong@hotmail.com, fhwang@imr.ac.cn

peened, ground down to 600#-SiC paper, and then ultrasonically cleaned in acetone prior to coating deposition.

2.2. Coatings Preparation

The nominal enamel composition, as given in Table 1, was designed and optimized by theoretical calculations using empirical equations proposed to predict enamel properties [27-28]. The enamel glaze was prepared by vitrifying the raw mineral mixture in proportion in air for about 10h at 1450°C with subsequent water quench. Instead of the conventional coarse enamel frit (20µm) [29], an ultrafine enamel frit with a mean size of 5µm was achieved by mechanical milling in order to decrease its sintering temperature [19]. In addition, the properties (sinterability, adherence, wettability, thermal stability) of the frit were further improved by introducing some additives, such as ZrO₂ (1-5wt.%), B₂O₃ (4-10wt.%), TiO₂ (1-3wt.%).

Table 1. Nominal Composition (wt.%) of Initial Enamel Frit

SiO ₂	Al ₂ O ₃	ZrO ₂	ZnO	Na ₂ O	K ₂ O	B ₂ O ₃	Balance
58.1	5.8	5.1	9.0	3.4	7.0	4.6	7.0

The ultrafine enamel frit was suspended within ethanol solution, and sprayed onto the sand-blasted substrates by means of an air-spraying process. Subsequently, the enamel frit layer was dried to remove ethanol completely at 100°C for around one hour. Finally, the bulk enamel coating was formed by vitrification in air at 900°C for 45min with a subsequent air cooling.

The Ti-35.45Al-20.05Cr (at.%) coating was also deposited on TiAlNb alloy by magnetron sputtering as a counterpart for comparison. The parameters of sputtering are described as follows, vacuum (6×10^{-3} Pa), sputtering power (2KW), argon flow rate and pressure (2.03sccm, 0.24Pa), and sputtering time (8h). According to EDS, the composition of sputtered TiAlCr coating is Ti-41.3Al-18.2Cr (at.%), which is slightly different from that of the initial target due to the difference in sputterability of the each component phase in the target material. The thickness of the two coatings (TiAlCr and enamel) is around 30µm.

2.3. Hot Corrosion Tests

Hot corrosion were carried out in 75 wt.% (Na, K)₂SO₄ + 25 wt.% NaCl melts at 750°C up to 60 hours. The examined specimens were completely immersed into the molten salts in Al₂O₃ crucibles with lids at 750°C in air for hot corrosion. The series, 30min, 5h, 10h, 15h, 25h, 40h, and 60h, were adopted as hot corrosion exposure time intervals in furnace. The specimens were removed from the furnace at regular intervals, cooled in air, washed in boiling water to remove the attached salts on the surfaces, dried in hot air, weighed by a balance with a precision of 10⁻⁵g. The corrosion kinetics was characterized with respect to the mass changes of examined specimens. In order to evaluate the probable dissolution of enamel into molten salts, the washing water was collected, and the contents of Ti, Al, Cr, Nb, and Si in the aqueous solutions were analyzed by chemical analysis.

2.4. Microstructure Characterization

The corroded specimens were protected by an electroless plating nickel film, mounted by epoxy, and characterized by scanning electron microscopy equipped by energy dispersive X-ray spectroscopy (SEM/EDS, FEG-SEM, Philips XL 305) to analyze surface corrosion products, cross sectional microstructure and interfacial reactions.

3. RESULTS

3.1. As-Vitrified Enamel Coatings

As shown in Fig. (1), the ultrafine enamel coating shows a compact structure and tightly mechanical bonding to the substrates of titanium alloys comparing with the conventional one [29]. The EDS results show that enamel coating consists of gray vitreous enamel matrix and white particles which are uniformly distributed in the matrix and enriched by ZrO₂, Al₂O₃ and MgO.

3.2. Corrosion Kinetics

Fig. (2) shows corrosion kinetics of Ti-based intermetallics with and without coatings in (Na, K)₂SO₄ + NaCl melts in air at 750°C. In case of the bare alloys, the kinetics of TiAl and Ti₃AlNb follow approximately linear law and TiAlNb shows the best corrosion resistance. The significant mass loss for TiAl indicates the low adherence and spallation characteristics of the corrosive products. The slightly decrease of weight of the bare TiAl specimen in the incubation period may result from the competition between the mass loss due to the volatility of chlorides and the mass gain by forming oxides during corrosion. Interestingly, the TiAlCr coating also shows rather poor corrosion resistance in the melts, and the mass gain of Ti₃AlNb and TiAlCr after corrosion for 60h is comparable. Despite of possessing the excellent oxidation resistance in air [7] and corrosion resistance in (Na, K)₂SO₄ melts [23], TiAlCr coating shows poor corrosion resistance in (Na, K)₂SO₄ + NaCl melts. This may be due to the formation of volatile chromium chlorides prior to forming protective oxide scale of Al₂O₃. The activity of aluminum is not enough to form a continuous and compact Al₂O₃ scale on TiAlCr due to the loss of chromium through chlorination during corrosion. In comparison with the bare alloys, the enamel coated alloys show much lower corrosion rate in cases of TiAl and Ti₃AlNb. However, the mass gain of the coated TiAlNb is slightly more than that of the bare alloy.

3.3. Hot Corrosion of Bare Alloys

As shown in Fig. (3), thick corrosive scales form on the bare alloys after corrosion for 60h in (Na, K)₂SO₄ + NaCl melts at 750°C. The corrosive products on TiAl can be divided into three layers which mainly consists of titania (gray layer), alumina (dark layer), and Al-depletion region (white gray layer) in order from outside to inside respectively. Also, many Al₂O₃ nodes (dark phase), even a thin band enriched by Al₂O₃ (the black line in Fig. 3a), are formed and embedded in the external TiO₂ layer, indicating competitive corrosion between Ti and Al. According to the kinetics (as shown in Fig. 2a), the non-protective layered products may be brittle and spalled due to the thermal cycle shock during corrosion.

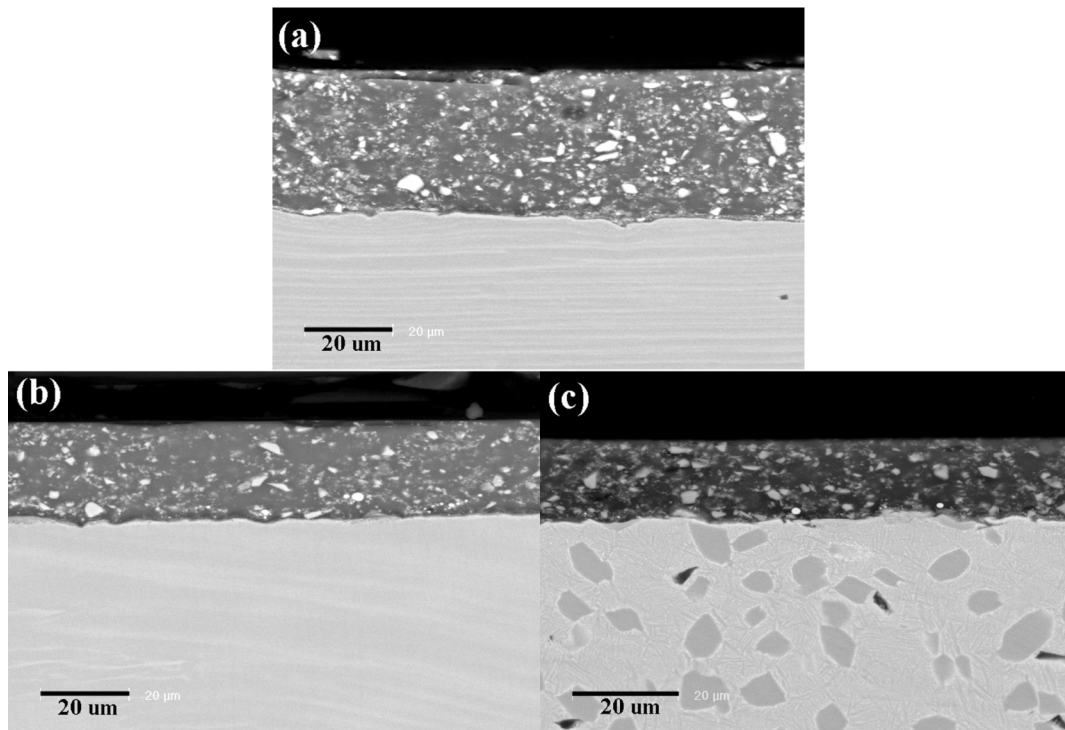


Fig. (1). The cross sectional microstructures of as-vitrified enamel coatings on (a) TiAl, (b) TiAlNb, and (c) Ti₃AlNb intermetallics.

As shown in Fig. (3b), a close view of the boxed region in Fig. (3a) and EDS analysis reveal the forming process of the corrosive scale on TiAl in the salt melts. The composition in the regions *I-III*, *A*, and *B* in Fig. (3b) is given in Table 2. The porous Al₂O₃ intermediate layer *I* may not inhibit the outwards diffusion of elements so that the high *S* content could be detected in the *Al*-depletion layer inbetween the *II* (rich in titanium chlorides) and *III* (rich in aluminum chlorides) regions. The increase of aluminum content from *II* to *A*, *B* regions indicates that the corrosion of aluminum is faster than that of titanium.

As shown in Fig. (3c), a relatively thin and compact Al₂O₃+TiO₂ oxide scale forms on TiAlNb alloys after corrosion. The doping of Nb in the scale could hinder the inward diffusion of corrosives (such as *S* with a content less than 1at.% in the scale). The increasing of Nb from outside to inside of the scale and its enrichment at the interface could improve the adhesion, protectiveness, and stabilization of the scale.

The relatively thick corrosion products on Ti₃AlNb can be divided into three layers (as shown in Fig. (3d)). The fraction of Al₂O₃ in the outer dark phase (*I*) is much higher than that in the other two layers (*II* and *III*). In addition, the content of Nb in the inner layer is relatively high in the inside layer (*III*). The composition of each layer is given in Table 3 according to EDS analysis. Although a high content of Nb could be detected in the corrosive scale (layer *I* and *II*), the voids and cracks form in the scale during corrosion, indicating poor adhesion of corrosive products. The substrate of Ti₃AlNb could not be protected by the previously formed scale.

3.4. Hot Corrosion of Coated Alloys

As shown in Figs. (4, 5), the interface stabilization of enamel coating in (Na, K)₂SO₄ + NaCl melts is associated

with the activity of aluminum on the substrates. The interface remains intact, and almost no clear interface reaction layer can be detected between enamel and Ti₃AlNb after corrosion as shown in Fig. (5). However, in case of the TiAl-based alloys (TiAl and TiAlNb), the interface reaction increases with the aluminum activity on the substrates. For example, the activity of aluminum in TiAl based alloys can be enhanced by doping Nb [10-13]. Thus, Fig. (4) shows that the thickness of reaction layer on TiAlNb (7.41μm) is thicker than the case of TiAl (5.17μm). EDS results show that the two interface reaction layers in case of TiAl-based alloys can be divided into three layers: a few oxides of Ti and Al doped in SiO₂ (*A* layer), Al₂O₃-based mixture (*B* layer), and *C* layer enriched by Ti with some diffusive voids. In case of TiAlNb, Nb can also be detected in the reaction layers.

It is worth noting that the enamel coating remains stable in the melts at 750°C regardless of the substrates. The chemical analysis results of the washing water indicate that no other enamel components could be detected except an extremely low content of Si and B (less than 0.5g/L).

As shown in Fig. (4d), besides the intergranular corrosion, a layered corrosive scale forms on the sputtered TiAlCr coating after corrosion. *A* is mainly composed of TiO₂, and *B* is enriched by Al₂O₃, followed by *C* layer of aluminum depletion and enrichment of sulfides (15.3 at.% S) with a few chlorine. Moreover, the interface corrosion between coating and substrate can be observed.

4. DISCUSSIONS

A continuous and compact Al₂O₃ scale is always expected to form on alloys during oxidation and corrosion as a barrier to protect the substrate against further corrosion of corrosives. In case of TiAl-based alloys, the higher activity

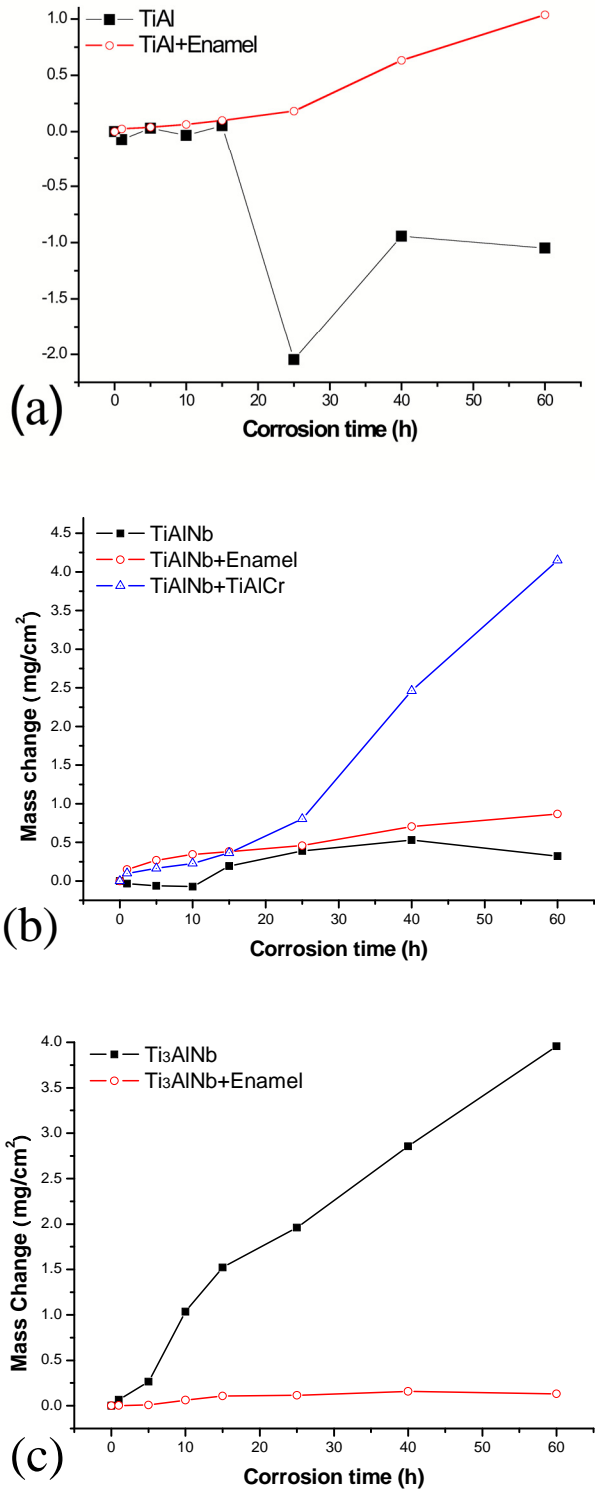


Fig. (2). Corrosion kinetics of (a) TiAl, (b) TiAlNb, and (c) Ti₃AlNb alloys with or without coatings in (Na, K)₂SO₄+NaCl melts at 750°C.

of aluminum is generally needed to obtain this protective scale through the selective oxidation of aluminum due to the similar oxygen appetency of Ti and Al [5, 6]. For example, the addition of Nb and Cr is one of the effective avenues to improve the formation of protective alumina by increasing

the activity of aluminum and the adhesion of oxides scale [7-14].

Nowadays, the TiAlCr coating has become one of the most promising protective coatings for Ti-based alloys from oxidation and hot corrosion. A continuous and compact Al₂O₃ scale is always expected to form on TiAlCr during oxidation in dry air and hot corrosion in sulfates melts due to the increasing activity of aluminum owing to the addition of Cr [7, 23]. However, it has been confirmed that the rapid degradation of TiAlCr coating would occur in the corrosive environment containing chlorine [22]. This is due to the formation of volatile chromium chlorides through a cyclic chlorination of Cr during hot corrosion at elevated temperature. Furthermore, it is observed that synergistic corrosion through chlorination and sulfidation of metals (Ti-based alloys and TiAlCr coating) occur in the mixture melts of SO₄²⁻ and Cl⁻ at 750°C in the present study.

As given in Table 4, the presumed thermochemical equilibriums of alloying elements (Ti, Al, and Cr) with molten salts ions (SO₄²⁻ group and Cl⁻ ion), and corresponding Gibbs energy changes and equilibrium constants can be calculated from the thermochemical data [30], except Eq.(1) due to the absence of data. In (Na, K)₂SO₄ + NaCl melts, because the dissolution and diffusion of oxygen are limited, the chemical equilibrium of sulfates decomposition to O₂, S₂, and oxidative SO₃ might proceed [25] (as revealed by Eq. 1-2 in Table 4) although Eq. (2) is thermodynamically difficult to happen.

As confirmed, selective oxidation of Al may take place under an extremely low oxygen partial pressure [31] to form Al₂O₃ scale on TiAl and TiAlNb in the salt melts. However, the chlorination of metallic components (Ti, Al, and Cr) may be more thermodynamically competitive, as shown in Eqs. (6), (11). As a result, Cl₂ would rapidly react with metals (Ti, Al, and Cr) to form volatile chlorides, as shown in Eqs. (7), (9), and (12). Subsequently, the chlorides (TiCl₄, AlCl₃, and CrCl₃) may be oxidized (TiO₂, Al₂O₃, and Cr₂O₃) to form chlorine gas (Eqs. 8, 10, and 13). Accordingly, the degradation of the alloys will be accelerated by the cyclic chlorination through the self catalysis of Cl₂. Similarly, the self catalysis of S₂ also plays an important role in the rapid depletion of Ti in alloys, as revealed in Eq. (3-5).

The corrosion kinetics of TiAl-based alloys depends on the competition between mass gain (oxidation and sulfidation) and mass loss due to the volatility of chlorides (chlorination) during hot corrosion at high temperature. The chlorination resulting in the volatility of AlCl₃ increases with the activity of aluminum in Ti-based alloys. As a result, no mass gain for TiAl but mass loss for TiAlNb in kinetics (as shown in Fig. (2)) are observable at the initial stage of corrosion. However, the mass gain increases with the oxidation of chlorides (Eqs. 8, 10, 13) and the sulfidation of metals (Eqs. 3, 5).

As mentioned above, the addition of Nb increases both the activity of aluminum and the adhesion of corrosive scale. Thus, TiAlNb shows the best corrosion resistance among the examined bare alloys due to the formation of a dense and adhesive scale enriched by Al₂O₃. Although the Al₂O₃-rich corrosive products form on TiAl under an extremely low oxygen partial pressure, the spallation of the scale leads to

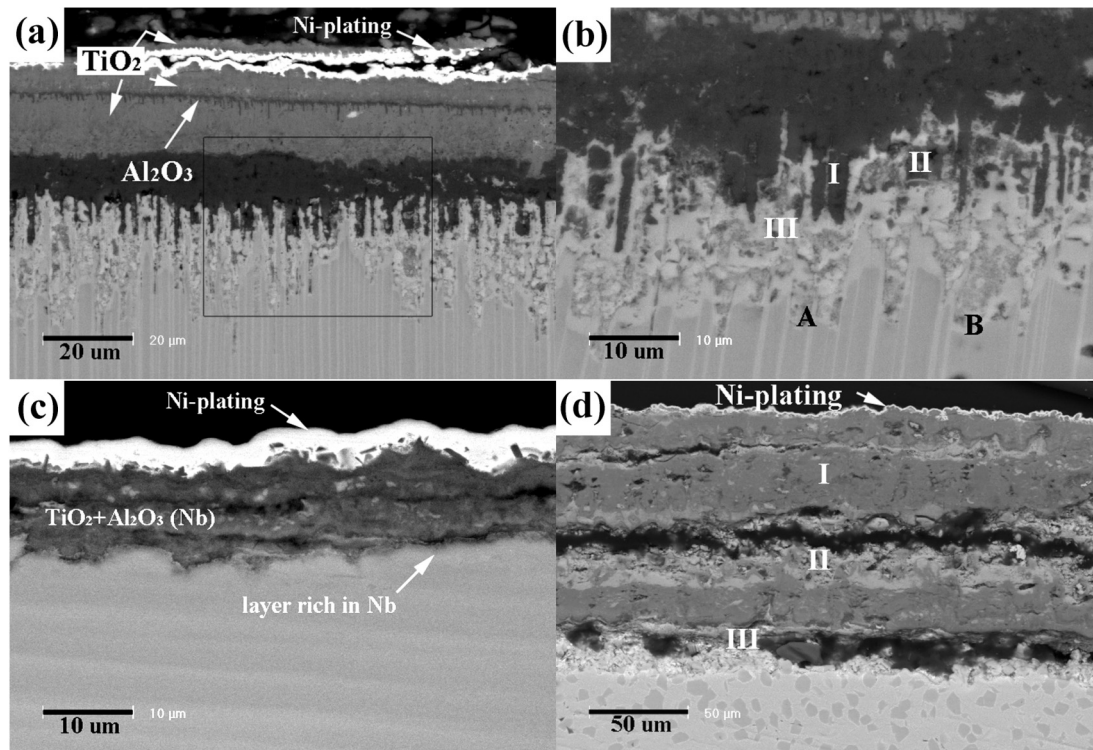


Fig. (3). Cross sectional microstructures of (a) TiAl, (c) TiAlNb, and (d) Ti_3AlNb bare alloys after hot corrosion for 60 hours in $(Na, K)_2SO_4 + NaCl$ melts at $750^\circ C$; and (b) close-view of the boxed interface in (a).

the rapid corrosion damage of the TiAl alloy. In case of Ti_3AlNb , the approximately linear law in the kinetics implies the rapid corrosion although the external corrosive scale exhibits a good adhesion to the substrate due to the doping of Nb. It is worth noting that the oxidation of Nb is difficult to occur due to the low oxygen partial pressure in the salt melts in spite of its high fraction (17at.%) in the alloy.

Table 2. EDS Analysis (at.%) of the Interface Between Scale and TiAl After 60h Corrosion (Fig. 3b)

	I	II	III	A	B
Ti	15.77	37.17	61.38	54.11	53.23
Al	32.7	29.17	3.27	40.94	42.78
S	4.1	15.16	23.65	1.74	1.46
O	47.43	18.5	11.7	3.21	2.53

Table 3. EDS Analysis (at.%) of Corrosion Products on Bare Ti_3AlNb After 60h Corrosion (Fig. 3d)

	O	Ti	Al	Nb	S	Cl	Na, K
I	34.2	18.73	7.49	3.13	10.73	1.62	24.1
II	41.5	14.04	3.21	19.3	7.6	0.83	13.52
III	19.09	16.83	2.84	22.89	9.55	0.97	27.83

Other than the excellent oxidation resistance of TiAlCr, its hot corrosion resistance in salt melts containing Cl^- ion is relatively poor. Not only the oxidation rate but also chlorination rate of aluminum increases with increasing its activity by adding Cr in the TiAl alloys. Moreover, the selective oxidation of aluminum is decreased due to chlorination of chromium and the volatility of chromium chlorides. As a result, the external scale on TiAlCr is mainly composed of the mixture of Al_2O_3 and TiO_2 . The corrosion kinetics of TiAlCr follows two linear laws indicating the variation of the corrosion mechanisms with increasing the exposure time. At the initial corrosion stage, the oxidation (mass gain) and chlorination (mass loss) of metallic elements in alloys are comparable resulting in a relatively small mass gain. The formation of corrosive products along the columnar intergranular boundary in the sputtered TiAlCr coating improves the adhesion of the external corrosion scale. However, the external scale could not significantly hinder the inward diffusion of corrosives (O , Cl^- , SO_4^{2-} and others) and outward volatility of chlorides due to its porous characteristics. Accordingly, although the formation of the scale enriched by Al_2O_3 further improves the protectiveness of the external corrosive scale from chlorination to a certain extent, the linear law in the corrosion kinetics implies that the synergistic corrosion of oxidation, sulfidation and chlorination of TiAlCr is the main corrosion mechanisms in the present environment (as depicted by equations in Table 4).

Although the enamel coating remains highly stable thermochemically in the salt melts according to the chemical analysis, the corrosives (O , Cl and S) may diffuse into the interface between enamel coating and Ti-based alloys

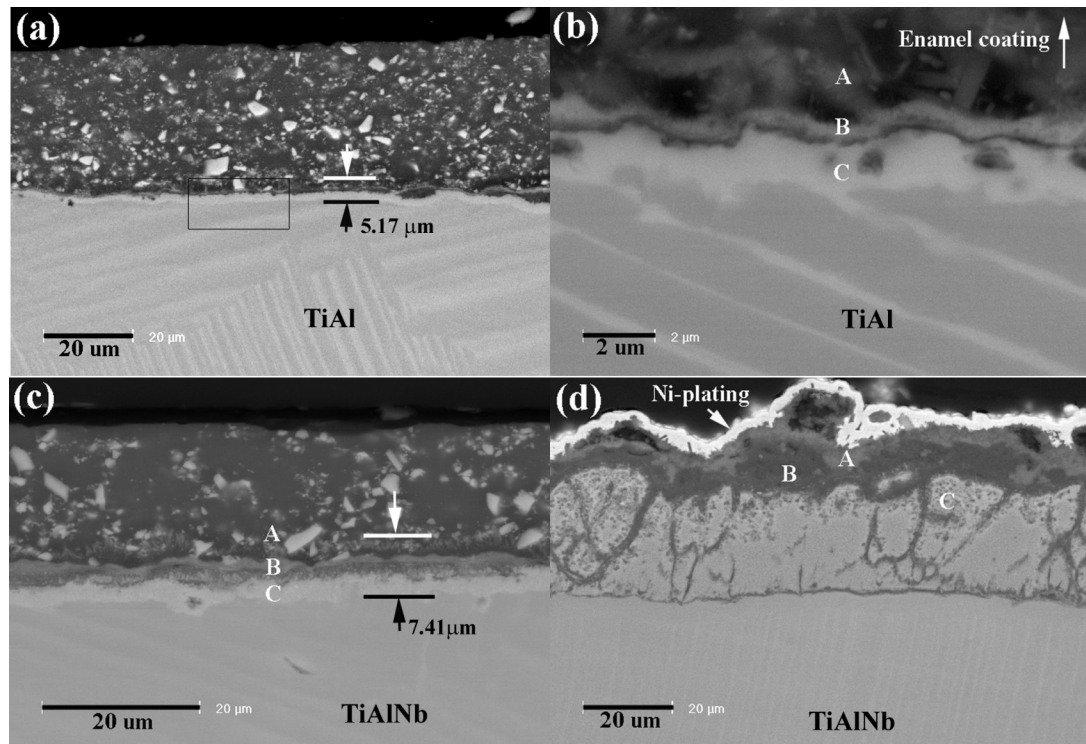


Fig. (4). Cross sectional microstructures of enamel coated (a) TiAl and (c) TiAlNb, and (d) TiAlCr coated TiAlNb alloys after hot corrosion in $(\text{Na}, \text{K})_2\text{SO}_4 + \text{NaCl}$ melts for 60h at 750°C ; and (b) close-view of the boxed interface in (a).

Table 4. Thermochemically Chemical Equilibrium Equations for Ti-Base Intermetallics in Molten $(\text{Na}, \text{K})_2\text{SO}_4 + \text{NaCl}$ Melts

No.	Equilibrium Equation	$\Delta G^0_{1023\text{K}}$	$\log K_{1023\text{K}}$
		(kJ.mol ⁻¹)	
1	$(\text{Na}, \text{K})_2\text{SO}_4(\text{l}) = \text{Na}_2\text{O}(\text{s}) + \text{K}_2\text{O}(\text{l}) + \text{SO}_3(\text{g})$	/	/
2	$\text{SO}_3(\text{g}) = 1/2\text{S}_2(\text{g}) + 3/2\text{O}_2(\text{g})$	228.1	-11.7
3	$\text{SO}_3(\text{g}) + \text{TiAl}(\text{s}) = \text{TiS}(\text{s}) + 1/2\text{Al}_2\text{O}_3(\text{s}) + 3/4\text{O}_2(\text{g})$	-567.8	29.0
4	$\text{TiS}(\text{s}) + \text{O}_2(\text{g}) = \text{TiO}_2(\text{s}) + 1/2\text{S}_2(\text{g})$	-571.7	29.2
5	$3\text{TiAl}(\text{s}) + \text{S}_2(\text{g}) = 2\text{TiS}(\text{s}) + \text{TiAl}_3(\text{s})$	-413.0	21.1
6	$\text{Ti}(\text{s}) + 2\text{NaCl}(\text{g}) + 3/2\text{O}_2(\text{g}) = \text{Na}_2\text{TiO}_3(\text{s}) + \text{Cl}_2(\text{g})$	-769.9	39.3
7	$\text{Ti}(\text{s}) + 2\text{Cl}_2(\text{g}) = \text{TiCl}_4(\text{g})$	-639.9	32.7
8	$\text{TiCl}_4(\text{g}) + \text{O}_2(\text{g}) = \text{TiO}_2(\text{s}) + 2\text{Cl}_2(\text{g})$	-118.6	6.1
9	$\text{Al}(\text{l}) + 3/2\text{Cl}_2(\text{g}) = \text{AlCl}_3(\text{g})$	-532.2	27.2
10	$2\text{AlCl}_3(\text{g}) + 3/2\text{O}_2(\text{g}) = \text{Al}_2\text{O}_3(\text{s}) + 3\text{Cl}_2(\text{g})$	-289.3	14.8
11	$\text{Cr}(\text{s}) + 2\text{NaCl}(\text{g}) + 2\text{O}_2(\text{g}) = \text{Na}_2\text{CrO}_4(\text{s}) + \text{Cl}_2(\text{g})$	-346.9	17.7
12	$2\text{Cr}(\text{s}) + 3/2\text{Cl}_2(\text{g}) = 2\text{CrCl}_3(\text{g})$	-653.5	33.4
13	$2\text{CrCl}_3(\text{g}) + 3/2\text{O}_2(\text{g}) = \text{Cr}_2\text{O}_3(\text{s}) + 3\text{Cl}_2(\text{g})$	-217.0	11.1

through some voids in the coatings. The interfacial reaction may occur. However, the oxidation may be the main interfacial reaction because the re-oxidation reaction of SiO_2 in enamel by aluminum in alloys tends to happen under the low partial pressure of oxygen at the interface. Thus, the interfacial reaction must be associated with the activity of aluminum at the interface. For example, the thickness of the interfacial reaction layer increases in order on Ti_3AlNb , TiAl, and

TiAlNb in terms of their activity of Al. Thus, the rapid selective oxidation of aluminum on TiAlNb under the low oxygen partial pressure at the interface may detach the enamel coating from the substrates due to the decrease of adhesion of coating. It is in good agreement with our previous report on the oxidation behavior of enamel coated TiAlNb alloys in air [20].

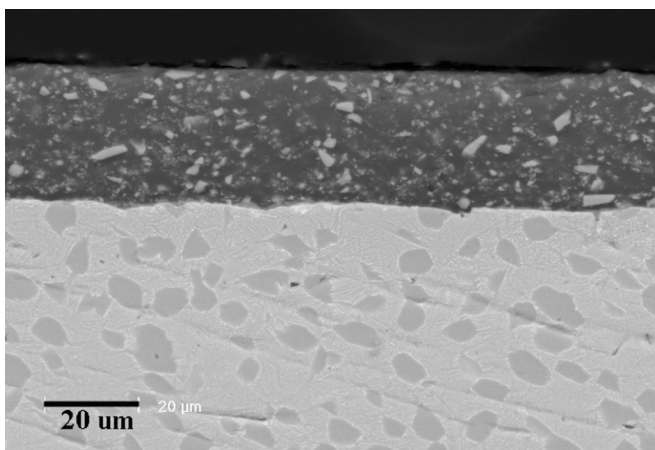


Fig. (5). Cross sectional microstructure of enamel coated Ti_3AlNb alloy after hot corrosion in $(Na, K)_2SO_4 + NaCl$ melts for 60h at $750^\circ C$.

5. CONCLUSIONS

In $(Na, K)_2SO_4 + NaCl$ melts at $750^\circ C$, the rapid corrosion damage of $TiAl$, $TiAlNb$, $TiAlCr$, and Ti_3AlNb bare alloys results from the self catalysis of sulfidation and chlorination of the metallic components. The mass loss at the initial corrosion stage is associated with the volatility of chlorides through the chlorination of metallic components. The $TiAlNb$ shows the best corrosion resistance in the melts among the three examined alloys due to the formation of adhesive scale enriched by Al_2O_3 . The rapid degradation of sputtered $TiAlCr$ coating is relevant to the chlorination of chromium and aluminum.

Enamel coating could protect Ti-base alloys from hot corrosion. In addition, the stability of enamel coatings on Ti-alloys decreases with increasing the activity of aluminum on the alloys during oxidation. This is due to the occurrence of reduction reaction of SiO_2 in enamel coating by aluminum under a low oxygen partial pressure at the interface of enamel/alloy.

REFERENCES

- [1] Craig BD. Handbook of Corrosion Data. 2nd ed. ASM International: Materials Park, OH 1995.
- [2] Austin CM. Current status of gamma Ti aluminides for aerospace applications. *Curr Opin Solid State Mater Sci* 1999; 4: 239-42.
- [3] Tetsui T. Gamma Ti aluminides for non-aerospace applications. *Curr Opin Solid State Mater Sci* 1999; 4: 243-8.
- [4] Loria EA. Gamma titanium aluminides as prospective structural materials. *Intermetallics* 2000; 8: 1339-45.
- [5] Meier GH, Appalonia D, Perkins RA, Chiang KT. Oxidation of High-Temperature Intermetallics. In: Grobstein T, Doychak J, Eds. *Proceedings of the Workshop on the Oxidation of High Temperature Intermetallics*; Warrendale, PA, USA: TMS; 1988; p. 185.
- [6] Becker S, Rahmel A, Schorr M, Schutze M. Mechanism of isothermal oxidation of the intermetallic $TiAl$ and of $TiAl$ alloys. *Oxid Met* 1992; 38: 425-64.
- [7] McCarron RL, Schaeffer JC, Meier GH, Berzits D, Perkins RA, Cullinan JR. Protective Coatings for Titanium Aluminide Intermetallics, Titanium '92. In: Froes FH, Caplan IL, Eds. *Proceedings of the Titanium 1992 Science and Technology Symposium*; Warrendale, PA: TMS; 1993; pp. 1971-8.

- [8] Brady MP, Smialek JL, Humphrey DL, Smith J. The role of Cr in promoting protective alumina scale formation by γ -based $Ti-Al-Cr$ alloys-II. Oxidation behavior in air. *Acta Mater* 1997; 45: 2371-82.
- [9] Fox-Rabinovic GS, Weatherly GC, Wilkinson DS, Kovalev AI, Wainstein DL. The role of chromium in protective alumina scale formation during the oxidation of ternary $Ti-Al-Cr$ alloys in air. *Intermetallics* 2004; 12: 165-80.
- [10] Chen G, Sun Z, Zhou X. Oxidation and mechanical behavior of intermetallic alloys in the $Ti-Nb-Al$ ternary system. *Mater Sci Eng A* 1992; 153: 597-601.
- [11] Yoshihara M, Miura K. Effects of Nb addition on oxidation behavior of $Ti-Al$. *Intermetallics* 1995; 3: 357-63.
- [12] Shida Y, Anada H. The effect of various ternary additives on the oxidation behavior of $Ti-Al$ in high-temperature air. *Oxid Met* 1996; 45: 197-219.
- [13] Perez P, Haanappel VAC, Stroosnijder MF. The effect of niobium on the oxidation behaviour of titanium in $N_2/20\% O_2$ atmospheres. *Mater Sci Eng A* 2000; 284: 126-37.
- [14] Brady MP, Smialek JL, Smith J, Humphrey JL. The role of Cr in promoting protective alumina scale formation by γ -based $Ti-Al-Cr$ alloys-I. Compatibility with alumina and oxidation behavior in oxygen. *Acta Mater* 1997; 45: 2357-69.
- [15] Shemet V, Tyagi AK, Becker JS, Lersch P, Singheiser L, Quadackers WJ. The formation of protective alumina-based scales during high-temperature air oxidation of $\gamma-Ti-Al$ alloys. *Oxid Met* 2000; 54: 211-35.
- [16] Copland EH, Gleeson B, Young DJ. Formation of $Z-Ti_{50}Al_{30}O_{20}$ in the sub-oxide zones of $\gamma-Ti-Al$ -based alloys during oxidation at $1000^\circ C$. *Acta Mater* 1999; 47: 2937-49.
- [17] Shemet V, Hoven H, Quadackers WJ. Oxygen uptake and depletion layer formation during oxidation of $\gamma-TiAl$ based alloys. *Intermetallics* 1997; 5: 311-20.
- [18] Zheng N, Fischer W, Grubmeier H, Shemet V, Quadackers WJ. The significance of sub-surface depletion layer composition for the oxidation behaviour of γ -titanium aluminides. *Scr Metall Mater* 1995; 33: 47-53.
- [19] Xiong Y, Zhu S, Wang F. The oxidation behavior and mechanical performance of $Ti60$ alloy with enamel coating. *Surf Coat Technol* 2005; 190: 195-9.
- [20] Xiong Y, Zhu S, Wang F. Effect of coatings on the isothermal and cyclic oxidation behaviors of $TiAlNb$ alloys at $800^\circ C$ in air. *Surf Coat Technol* 2005; 197: 322-6.
- [21] Xiong Y, Zhu S, Wang F, Lee C. The effect of enamel coating on the oxidation behavior of Ti_3Al -based intermetallics at $750^\circ C$ in air. *Mater Sci Eng A* 2007; 460-461: 214-9.
- [22] Xiong Y, Zhu S, Wang F. Synergistic corrosion behavior of coated $Ti60$ alloys with $NaCl$ deposit in moist air at elevated temperature. *Corros Sci* 2008; 50: 15-22.
- [23] Tang Z, Wang F, Wu W. Effect of a sputtered $Ti-Al-Cr$ coating on hot corrosion resistance of gamma- $Ti-Al$. *Intermetallics* 1999; 7: 1271-4.
- [24] Zhang K, Li Z, Gao W. Hot corrosion behaviour of $Ti-Al$ based intermetallics. *Mater Lett* 2002; 57: 834-43.
- [25] Tang Z, Wang F, Wu W. Hot-corrosion behavior of $Ti-Al$ -base intermetallics in molten salts. *Oxid Met* 1999; 51: 235-50.
- [26] Zhang K, Gao W, Liang J. Influence of Y-addition on the oxidation behavior of Al-rich $\gamma-Ti-Al$ alloys. *Intermetallics* 2004; 12: 539-44.
- [27] Fetterolf LD, Parmelee CW. The effects of soda barium, and zinc on the elasticity and thermal expansion coefficients of glass I. *J Am Ceram Soc* 1929; 12: 193-216.
- [28] Gou W. Calculations of Enamel Glaze (in Chinese). Report of the Chinese Chongqing Ceramic Society 1964.
- [29] Xiong Y, Wang F, Niu Y, Wu W. Effect of enamel coating on the corrosion of $Ti60$ alloy. *Mater Sci Forum* 2001; 369-72: 743-50.
- [30] Barin I. *Thermochemical Data of Pure Substances*. 2nd ed. VCH: Weinheim 1993.
- [31] Yoshihara M, Tanaka R, Suzuki T, Shimizu M. In: Johnson LA, Stigler JO, Eds. *High Temperature Ordered Intermetallic Alloys*. MRS: Pittsburgh, PA 1991; Vol. IV: p. 975.